

Title	Reentrant cone angle dependence of the energetic electron slope temperature in high-intensity laser-plasma interactions
Author(s)	Nakatsutsumi, M.; Kodama, R.; Norreys, P. A. et al.
Citation	Physics of Plasmas. 2007, 14(5), p. 050701
Version Type	VoR
URL	https://hdl.handle.net/11094/2888
rights	
Note	

Osaka University Knowledge Archive : OUKA

<https://ir.library.osaka-u.ac.jp/>

Osaka University

Reentrant cone angle dependence of the energetic electron slope temperature in high-intensity laser-plasma interactions

M. Nakatsutsumi,¹ R. Kodama,^{1,2} P. A. Norreys,³ S. Awano,¹ H. Nakamura,¹ T. Norimatsu,² A. Ooya,^{1,2} M. Tampo,² K. A. Tanaka,^{1,2} T. Tanimoto,¹ T. Tsutsumi,¹ and T. Yabuuchi¹

¹Graduate School of Engineering, Osaka University, 2-1 Yamada-oka, Suita, Osaka 565-0871, Japan

²Institute of Laser Engineering, Osaka University, 2-6 Yamada-oka, Suita, Osaka 565-0871, Japan

³Rutherford Appleton Laboratory, Chilton, Didcot, Oxfordshire OX11 0QX, United Kingdom

(Received 26 January 2007; accepted 22 March 2007; published online 14 May 2007)

Energy spectra of fast electrons, generated when high-intensity laser pulses irradiated hollow conical targets, have been measured experimentally. It is shown here that the slope temperature of the fast electrons is strongly dependent on the opening angle of the cone, and has a maximum value at 25°. The data confirms optical guiding of the laser pulse, by comparison of the measured electron temperature with ray-tracing calculations that include absorption in plasmas. The enhanced energy flow and intensity induced by optical guiding of the laser pulse inside the cone as a function of the opening angle as well as the f -number of the focusing optics is discussed. © 2007 American Institute of Physics. [DOI: 10.1063/1.2730490]

The rapid development of high-intense laser systems, both in terms of the available energy and the power that can be focused onto a target, provides many new opportunities for studies in high energy density science. These include the fast ignition approach (FI) to inertial confinement fusion,¹ medical science,² laboratory astrophysics,³ equation of state,⁴ etc.

The FI scheme allows the compression of the deuterium-tritium fuel to be separated from the heating phase. The heating is then caused by the stopping of large numbers of fast electrons or ions that are generated during an ultra-intense laser-plasma interaction. The crucial issue of this concept is the transfer of energy from the laser pulse to the compressed plasma. At peak compression there is still some distance between the fusion fuel and the critical density surface. A hole-boring scheme has been proposed as a method of pushing the critical density surface closer to the compressed fuel and to provide a propagation channel through the long scale length coronal plasma for the ultra-intense laser pulse.⁵ Alternatively, the reentrant-cone concept, where a hollow gold cone is inserted into a spherical shell, has been proposed as a method of avoiding plasma instability growth in the coronal plasma.⁶ A significant increase in the yield of thermal fusion neutrons was observed with this configuration.⁷ In addition, indirectly driven implosion using reentrant-cone shell target have also investigated.⁸ A recent study with three-dimensional particle-in-cell simulations has shown that the laser pulse at the cone tip can be up to 20 times more intense compared to that at the inlet plane; in addition, the surface electron flow is also confined in a plasma skin layer by self-generated quasistatic magnetic fields that are coupled with the electrostatic sheath field.⁹ The energetic electron and proton production from hollow-cone targets was also investigated experimentally; a higher number of fast electrons, as well as an increased accelerated proton cutoff energy, was obtained with an opening angle of 30°, compared to 60°.¹⁰ However, no systematic studies have yet been made to opti-

mize the cone shape; e.g., the opening angle of the cone.

In this letter, the opening angle dependence of hollow cone-foil targets for relativistic electron production is described and the optimum cone geometry to achieve high energy concentration at the cone tip is presented. The experimental results show that the temperature of the accelerated electrons derived from the slope of the electron distribution measured at the chamber wall (which is related to the intensity of the laser light at the cone tip) is strongly dependent on the opening angle of the cone. Ray-tracing calculations have been performed to estimate the enhancement of the light intensity and the energy concentration at the tip of the cone that confirms optical guiding. The calculations also suggest that the optimum opening angle is related to the f -number of the laser focusing optics. Good agreement is found between this model and the experimental results.

The experiment was performed using a 20 TW Nd-glass laser system that delivered 700 fs pulses with a wavelength of 1053 nm, and a maximum energy of approximately 10 J on target.¹¹ The front end of this system consisted of an optical parametric chirped pulse amplification preamplifier and created a pulse with an intensity contrast ratio of 10^{-8} .¹² The s -polarized pulse was focused using an $f/3.8$ off-axis parabola at an incidence angle of 4° onto the target (to avoid any back-reflection of the incident laser light into the laser chain). The focal spot size was $25 \pm 5 \mu\text{m}$ full width at half maximum (FWHM). The intensity on target was typically $2 \times 10^{18} \text{ W cm}^{-2}$.

The targets consisted of a hollow-glass cone attached to a plane solid Al slab [see Figs. 1(a) and 1(b)]. The Al slab had a thickness of 10 μm and size of 500 $\mu\text{m} \times 500 \mu\text{m}$. It was attached to the cone via a glue joint with 4° to the cone axis normal. The laser axis was same as the cone axis. The hollow diameter at the cone tip was 15 μm . The opening full angles of the cones were varied from 8° to 60°. An electron spectrometer was deployed directly along the laser axis to detect the fast electron energy spectra generated by the laser-

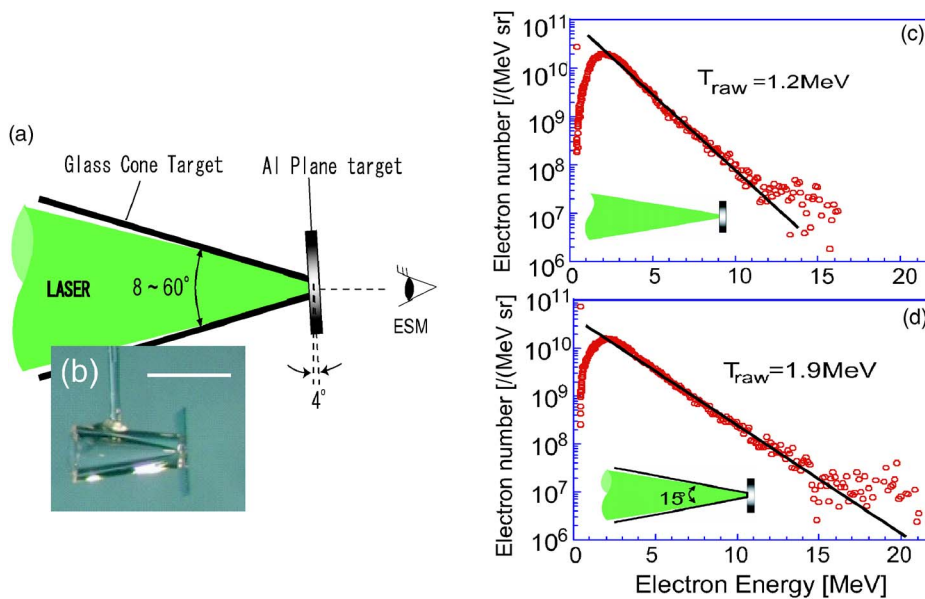


FIG. 1. (Color online) (a) Schematic layout of the experimental setup. The energy spectra of the fast electrons produced by laser-solid interactions were measured using the electron spectrometer. (b) The picture of the target. The white scale bar indicates $500\ \mu\text{m}$. (c) and (d) Typical spectra of electron energy obtained from (c) plane Al foil without cone (open geometry) (d) plane Al foil with a hollow cone attached that had an opening angle of 15° .

plasma interaction. The electron spectrometer consisted of a pair of permanent magnets producing a uniform magnetic field of $4.5\ \text{kG}$. A Fujifilm imaging plate (IP)—type BAS-SR2025—was used to detect the fast electrons. The IP is a time-integrated detector making use of the photostimulated luminescence (PSL) effect. The electrons first passed through the collimating hole (which was $5\ \text{mm}$ in diameter) when entering the spectrometer and then traversed the magnetic field region. The electron trajectories were bent by this magnetic field and were recorded on the IP whose location was determined by the electron Larmor radius. The calibration of the IP used to obtain the absolute electron numbers from the PSL values (which was the signal intensity displayed by the readout system) is described in Ref. 13. The entrance to the collimator and the magnetic field region were located 85 and $124.8\ \text{cm}$ from the target at the chamber center, respectively. The obtained energy spectra are fitted with a Boltzmann-like distribution to obtain the slope temperatures. Typical electron energy spectra obtained with the different kinds of target structures are shown in Figs. 1(c) and 1(d): (c) is a plane Al foil without cone (open geometry) and (d) is a plane Al foil with a hollow cone attached that had an opening angle of 15° . Since there were shot-to-shot fluctuations in the laser energy delivered to target, the laser intensity in the open geometry ranged from 1.5×10^{18} to $3 \times 10^{18}\ \text{W cm}^{-2}$. To take this intensity fluctuation into account, the obtained electron temperature was corrected using the intensity scaling of the temperature ($T \propto I^{0.5}$) determined by Pukhov,¹⁴ i.e.,

$$T_{\text{correction}} = T_{\text{raw}} \times \sqrt{2 \times 10^{18} [\text{W cm}^{-2}] / I},$$

where T_{raw} is the raw temperature and I is the laser intensity in the open geometry. The corrected temperature in Fig. 1 is (c) $T_{\text{correction}} = 1.0\ \text{MeV}$ (open geometry) and (d) $T_{\text{correction}} = 2.1\ \text{MeV}$ (cone) that correspond to a raw temperature of (c) $T_{\text{raw}} = 1.2\ \text{eV}$ and (d) $T_{\text{raw}} = 1.9\ \text{MeV}$, respectively [the intensities on the open geometry were (c) $3 \times 10^{18}\ \text{W cm}^{-2}$, (d) $1.6 \times 10^{18}\ \text{W cm}^{-2}$]. Figure 2 shows the $T_{\text{correction}}$ versus the opening angle of the cone. The big circles are the experimen-

tal data points. The horizontal dotted line indicates the temperature obtained with the open geometry. The results show, the temperatures strongly depend on the opening angle of the cone and have a maximum value at 25° . The error bars are defined by taken account of the scattering of the data from the Boltzmann fitting curve of the electron energy spectra. The small circles and lines are calculation, which is described in the next section.

There is some uncertainty on how the electron tempera-

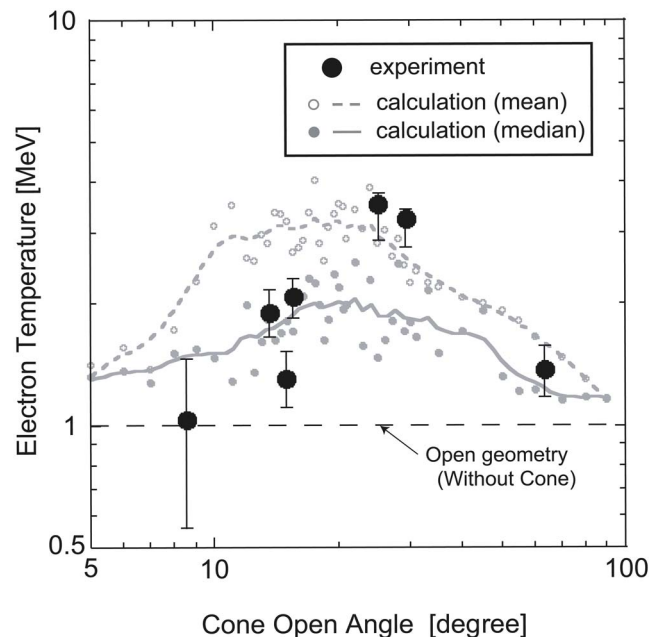


FIG. 2. Electron slope temperatures vs opening angle of the cone. The big circles are the experimental data points $T_{\text{correction}}$. The small circles are given by the ray-trace calculations and lines are the smoothed fit to these points. The calculated light intensities at the cone tip are converted to the temperatures assuming $T \propto I^{0.5}$. The intensities are expressed in two ways: either as the mean (open circles), or as the median (closed circles) of the local intensities at the tip.

ture measured with an electron spectrometer set far from the target relates to the electron distribution generated in the laser-plasma interaction itself. The spectra are likely to be influenced by electrostatic fields that build up on the target surfaces and prevent further escape of electrons. The electrostatic fields are known to accelerate ions via the sheath field mechanism, particularly protons. These electrostatic fields could potentially skew the electron distribution measured at the chamber wall so that the temperature measured there might not reflect the electron distribution inside the target during the interaction. However, the energy transfer to the proton beams (and therefore the electrostatic fields) remains relatively small at these intensities.¹⁵ In addition, it was shown by Malka and Miquel¹⁶ that the electron temperatures derived from fitting Boltzmann-like distributions to the electron spectra measured there can be related to the fast electron temperature of the laser-plasma interaction.

The results presented here clearly show that the temperature of the fast electrons is strongly dependent on the opening angle of the cone. They suggest that the laser light is optically guided by a plasma mirror¹⁷⁻¹⁹ generated on the inner walls of the cone and that the intensity at the cone tip is enhanced. When a sufficiently intense laser is incident inside the cone, ionization takes place on the leading edge of the pulse and the rest of the laser pulse then interacts with the plasma formed there. The very rapid increase in the reflectivity at the cone wall as the plasma mirror is formed there then acts to reflect most remaining energy to the tip of the cone.^{9,10} The intensity at the cone tip was calculated using a ray-tracing model, in which the incident rays were specularly reflected at the cone wall by the plasma mirror and had straight trajectories between reflections. The reflectivity was calculated by dividing the laser fraction into *s*- and *p*-polarization interactions. Take into account the laser intensity on the cone wall is estimated as from 10^{16} to 5×10^{17} W/cm² in the experiment, the reflectivity for the *s*-polarized component (i.e., the *E*-field of the laser pulse is perpendicular to the plane containing the density gradient and the Poynting vector) was assumed to be 70% at all angles of incidence based on the similar intensity experiment.¹⁷ For the *p*-polarized component, relatively lower reflectivity is predicted,¹⁸ the incident angle-dependent reflectivity was taken from the calculations by Gibbon and Bell.²⁰ The distribution of the incident beam was defined to have an Airy pattern and focused by an *f*/3.8 optics at the tip with the FWHM of the first central maximum of 30 μ m. Since the focal spot was measured to have a non-negligible energy spread out over many times the ideal spot size in this experiment, the Airy pattern was superimposed onto a background level such that only 30% of the incident laser energy was contained within the FWHM of the first central maximum. No energy outside the five times of FWHM (=150 μ m) was assumed. The temporal evolution of the plasma was not included in this calculation. To take account of the differences in the optical path length of the different rays, the phase of each ray was also included in this model. The local field amplitude *E* at the cone tip was given by the superposition of each ray's complex field amplitude including phase; then obtain the local intensity by EE^* , where E^* is

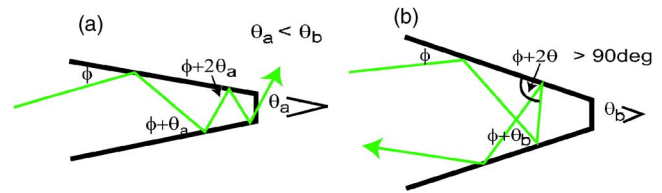


FIG. 3. (Color online) Light guiding inside the cone target with different opening angles: (a) small angle and (b) large angle.

the complex conjugate amplitude of *E*. The intensity in the cone tip consists of a speckle pattern with locally sharp “hot spots” superimposed on this pattern. Consequently, the overall intensity at the tip in Fig. 2 is expressed in two ways: either as the mean intensity itself, or as the median of the intensity. The mean intensity plot includes contributions from the entire pattern at the cone tip, but this can be skewed upwards by the hot spots in the intensity pattern there. On the other hand, the median always gives the typical intensity closer to the speckle level, but neglects those intensities in the hot spots that might contribute to the electron acceleration process. The open and closed small circles in Fig. 2 are the mean and median values for individual calculations of the opening angle. Assuming $T \propto I^{0.5}$, the calculated intensities were converted to the temperatures. The fluctuations are the result of phase effects. The dotted and solid lines are the smoothed fit to these points. The experimental results are bounded by these two calculations and can be explained as follows (see Fig. 3). After each reflection inside the cone, ϕ changes to $\phi + \theta$, where the θ is the cone angle and ϕ is the angle between the ray and the cone wall at a reflecting point. After some reflections when the injection angle exceeds the critical value of $\phi = 90^\circ$, the light will be diverted back toward the cone entrance [Fig. 3(b)], causing energy loss. On the other hand, when the cone angle is smaller than the laser focusing angle which is defined by numerical aperture of the focusing optics, some portion of the light cannot enter the cone and this also causes energy loss. These two limits suggest that an optimum angle of the cone for efficient optical guiding exists. The calculations confirm that it was between 10° – 25° .

It should be also noted that the opening angle dependence of laser light guiding will change with the experimental conditions, particularly the *f*-number of the focusing optics. Figure 4(a) shows the mean intensity at the cone tip normalized to the intensity in the open geometry. The solid line is a calculation for the *f*/3.8, while the broken line is for the *f*/8. The result shows that the optimum angle for the effective intensity at the tip is clearly dependent on the *f*-number of the focusing optics: 5° – 10° for *f*/8, 10° – 25° for *f*/3.8. The fraction of the total input energy arrived to the cone tip was also calculated [see Fig. 4(b)]. The calculation of the fraction is averaged value at the tip, which takes into account of the absorption at the side wall but no phase effect at the tip. The result shows the maximum fraction at 10° for the *f*/8 and 25° for the *f*/3.8. The optimum angles for the energy fraction at the tip could be different from the angles for the intensity maximum as shown in Figs. 4(a) and 4(b). This difference in the optimization of the cone angle should

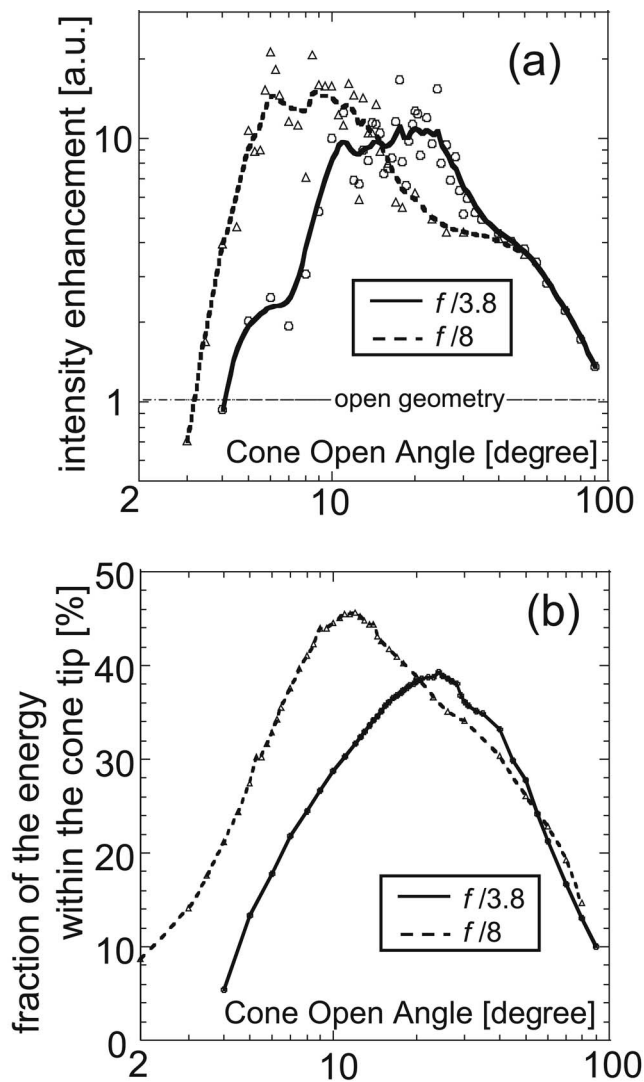


FIG. 4. (a) Mean intensity at the cone tip with different f -number of the incident laser. (b) Fraction of the incident laser energy within the cone tip.

be useful for applications such as FI target design, which would require higher energy fraction and lower intensity at the tip of the cone.

In summary, the energy spectra of fast electrons produced by the hollow cone attached targets have been experimentally investigated. The results show that the fast electron temperature is strongly dependent on the opening angle. This cone geometry dependence can be explained by the intensity enhancement at the tip which has been confirmed by a ray-tracing model. The experiments are consistent with these simple calculations, indicating that the effective intensity and energy fractions of the laser light at the cone tip are optimized by the opening angle. In addition, the cone angle dependence of the light guiding also changes with the f -number of the focusing optics. Future work will need to

concentrate on the effect of the pulse duration, particularly as FI requires a pulse duration an order of magnitude larger than those reported here.

ACKNOWLEDGMENTS

The authors are thankful to K. Sawai, K. Suzuki, Y. Miyazaki, K. Okabe, and T. Sera of the GMII operating group, and Y. Kimura and T. Sudo of the target fabrication group.

This research is supported by the project of "high energy density plasma photonics" under the Core Research for Evolutional Science and Technology (CREST), Japan Science and Technology Agency.

- ¹M. Tabak, J. Hammer, M. E. Glinsky, W. L. Kruer, S. C. Wilks, J. Woodworth, and E. M. Campbell, *Phys. Plasmas* **1**, 1626 (1994); P. A. Norreys, R. Allot, R. J. Clarke *et al.*, *Phys. Plasmas* **7**, 3721 (2000); M. Key, *Nature (London)* **412**, 775 (2001); R. Kodama, K. Mima, K. A. Tanaka *et al.*, *Phys. Plasmas* **8**, 2268 (2001).
- ²I. Spencer, K. W. D. Ledingham, R. P. Singhal *et al.*, *Nucl. Instrum. Methods Phys. Res. B* **183**, 449 (2001); K. W. D. Ledingham, P. McKenna, and R. P. Singhal, *Science* **300**, 1107 (2003); S. Fritzler, V. Malka, G. Grillon *et al.*, *Appl. Phys. Lett.* **83**, 3039 (2003).
- ³B. A. Remington, D. Arnet, R. P. Drake, and H. Takabe, *Science* **284**, 1488 (1999); J. M. Foster, B. H. Wilde, P. A. Rosen *et al.*, *Astrophys. J. Lett.* **634**, L77 (2005); M. Koenig, T. Vinci, A. Benuzzi-Mounaix *et al.*, *Phys. Plasmas* **13**, 056504 (2006).
- ⁴R. Cauble, L. B. Da Silva, T. S. Perry *et al.*, *Phys. Plasmas* **4**, 1857 (1997); G. W. Collins, P. Celliers, L. B. Da Silva *et al.*, *Phys. Plasmas* **5**, 1864 (1998); A. Benuzzi-Mounaix, M. Koenig, G. Huser *et al.*, *Phys. Plasmas* **9**, 2466 (2002); N. Ozaki, T. Ono, K. Takamatsu *et al.*, *Phys. Plasmas* **12**, 124503 (2005).
- ⁵R. Kodama, K. Takahashi, K. A. Tanaka, M. Tsukamoto, H. Hashimoto, Y. Kato, and K. Mima, *Phys. Rev. Lett.* **77**, 4906 (1996); A. Pukhov and J. Meyer-ter-Vehn, *Phys. Rev. Lett.* **79**, 2686 (1997).
- ⁶R. Kodama, P. A. Norreys, K. Mima *et al.*, *Nature (London)* **412**, 798 (2001).
- ⁷R. Kodama, H. Shiraga, K. Shigemori *et al.*, *Nature (London)* **418**, 933 (2002).
- ⁸R. Stephans, S. P. Hatchett, R. E. Turner, K. A. Tanaka, and R. Kodama, *Phys. Rev. Lett.* **91**, 185001 (2003).
- ⁹Y. Sentoku, K. Mima, H. Ruhl, Y. Toyama, R. Kodama, and T. E. Cowan, *Phys. Plasmas* **11**, 2083 (2004).
- ¹⁰R. Kodama, H. Azechi, H. Fujita *et al.*, *Nucl. Fusion* **44**, S276 (2004); Z. L. Chen, R. Kodama, M. Nakatsutsumi *et al.*, *Phys. Rev. E* **71**, 036403 (2005).
- ¹¹Y. Kitagawa, R. Kodama, K. Takahashi *et al.*, *Fusion Eng. Des.* **44**, 261 (1999).
- ¹²H. Yoshida, E. Ishii, R. Kodama *et al.*, *Opt. Lett.* **28**, 257 (2003).
- ¹³K. A. Tanaka, T. Yabuuchi, T. Sato *et al.*, *Rev. Sci. Instrum.* **76**, 013507 (2005).
- ¹⁴A. Pukhov, Z.-M. Sheng, and J. Meyer-ter-Vehn, *Phys. Plasmas* **6**, 2847 (1999).
- ¹⁵A. P. Fews, P. A. Norreys, F. N. Beg, A. R. Bell, A. E. Danger, C. N. Danson, P. Lee, and S. J. Rose, *Phys. Rev. Lett.* **73**, 1801 (1994).
- ¹⁶G. Malka and J. L. Miquel, *Phys. Rev. Lett.* **77**, 75 (1996).
- ¹⁷Ch. Ziener, P. S. Foster, E. J. Divall, C. J. Hooker, M. H. R. Hutchinson, A. J. Langley, and D. Neely, *J. Appl. Phys.* **93**, 768 (2003).
- ¹⁸G. Doumy, F. Quéré, O. Gobert *et al.*, *Phys. Rev. E* **69**, 026402 (2004).
- ¹⁹B. Dromey, S. Kar, M. Zepf, and P. Foster, *Rev. Sci. Instrum.* **75**, 645 (2004).
- ²⁰P. Gibbon and A. R. Bell, *Phys. Rev. Lett.* **68**, 1535 (1992).